Supporting Information

Toward the Electrochemical Valorization of Glycerol: Fourier Transform Infrared Spectroscopic and Chromatographic Studies

Yaovi Holade, Cláudia Morais*, Karine Servat, Teko W. Napporn and K. Boniface Kokoh

Université de Poitiers, IC2MP CNRS UMR 7285, 4 rue Michel Brunet – B27, BP 633, 86022 Poitiers cedex, France

*corresponding author: claudia.gomes.de.morais@univ-poitiers.fr

1- Physicochemical data about the synthesized catalyst by "Bromide Anion Exchange Method"

Table S1: Lattice parameter (a), metal loading (wt. %), crystallites (L_v), particles size (d_{TEM}), of the catalytic particles as determined by TGA, XRD, TEM respectively for PdM/C (M = Ni or Ag).

Pd:M atomic ratio		100:0	90:10	80:20	70:30	60:40	50:50	30:70	0:100
PdNi/C	**a / Å**	3.91	3.92	3.92	3.92	3.91	3.91	/	/
	L_V / nm	4.1	3.2	3.3	3.2	2.8	3.6	/	/
	(wt. %)	29	29	25	30	30	26	30	30
	d_{TEM} / nm	3.7	/	/	/	3.7	/	/	/
PdAg/C	**a / Å**	3.91	3.95	3.95	4.00	3.99	4.03	4.06	4.09
	L_V / nm	4.1	3.5	3.8	3.0	3.2	3.6	6.4	39.5
	(wt. %)	29	28	29	25	24	26	29	24
	d_{TEM} / nm	3.7	/	4.0	/	/	/	/	/

2- Successive cyclic voltammograms of $Pd_{30}Ag_{70}$/C electrode

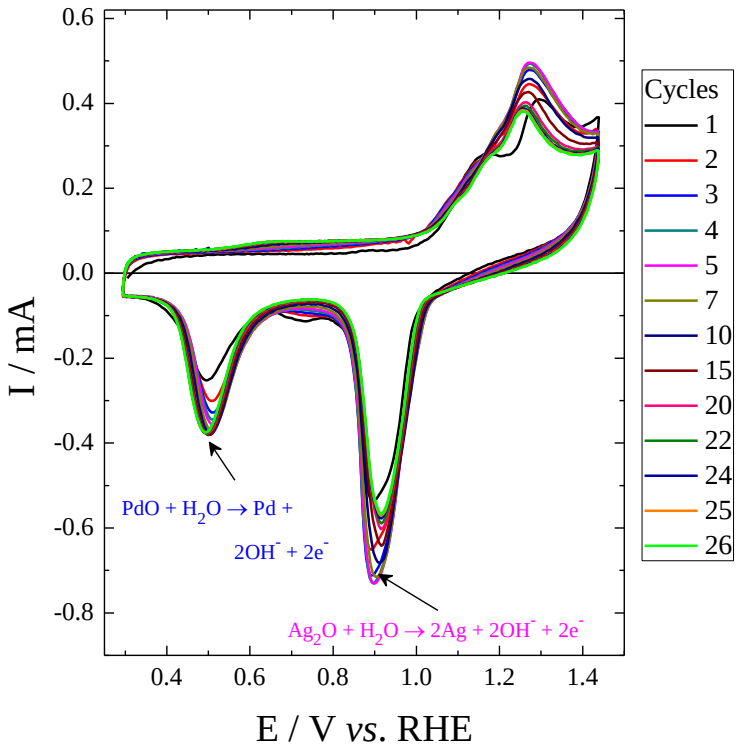

Figure S1: Successive cyclic voltammograms of $Pd_{30}Ag_{70}$/C electrode recorded in 0.1 mol L^{-1} NaOH at 50 mV s^{-1}.

3- Description of the method used for specific electrochemical surface area (SECSA) evaluation.

Various methods can be used to evaluate the electrochemical active surface are of metal: adsorption/desorption of hydrogen, stripping of probe molecule (CO), stripping of under potential deposition (UPD) or reduction of oxide.[1-4] It is well-known that Pd (more especially NPs) has an ability to absorb hydrogen into its crystal lattice. [5-10] To avoid this phenomenon, we used the reduction peak of palladium oxide (PdO). Silver does not present hydrogen region as can be seen in figure S4(b). A charge density of 424 μC cm^{-2} ($Q_{monolayer}$) was associated to the reduction of the formed PdO monolayer.[11,12] For the reduction of Ag_2O

monolayer, this charge was 420 μC cm^{-2} ($Q_{monolayer}$).[13] Because of the presence of $Ni(OH)_2$ species in the PdNi/C catalysts, it is not possible to evaluate their active surface areas.[14] The figure S4 shows the integrated region. The exchange charge ($Q_{exchanged\ charge}$) was obtained by using Eq. (2) on Origin8® software. But for confirmation, we used the old method named "weighing method" to get this exchange charge. This method use tracing paper. Briefly, it involves cutting a known surface of tracing paper and to weigh it. This charge is calculated by using the Eq. (3) that we do not develop it establishment. The variables a, b, *x*, *y* and *v* used in Eq. (3) are represented on figure S4(c); s_0 is the surface of the tracing paper which is cut. The variable m_0 is the weight of the tracing paper while m_1 is the weight of the shaded curve printed on any paper.

$$\mathrm{SA}\ (\mathrm{cm}^2) = \frac{Q_{exchangedcharge}(\mu C)}{Q_{monolayer}(\mu C\ cm^{-2})} \qquad \text{(Eq. 1)}$$

$$Q_{exchangedcharge}(\mu C) = \frac{1}{v(mV\ s^{-1})}\left(\int_{E_{onset}}^{E_{end}} i(E)dE\right),\ i(\mu A)\ \text{and}\ E(mV) \qquad \text{(Eq. 2)}$$

$$Q_{exchangedcharge} = \frac{1}{v(mV\ s^{-1})}\left(\frac{m_1}{m_0}\times\frac{s_0}{x\times y}\times\frac{a\times b}{v}\right) \qquad \text{(Eq. 3)}$$

$$\mathrm{SECSA}(m^2 g^{-1}) = \frac{\mathrm{SA}\ (m^2)}{\text{Total metal weight (g)}} \qquad \text{(Eq. 4)}$$

$Q_{monolayer}$ is associated to the reduction of the complete first oxide monolayer to free metallic. The Eq. (4) serves to get SECSA in $\mathbf{m^2\ g^{-1}}$ while Eq. (5) was used to obtain SECSA in $\mathbf{m^2\ g^{-1}_{Pd}}$. The latter is used to express the active surface area by the noble metal weight.

$$\mathrm{SECSA}(m^2 g_{Pd}^{-1}) = \frac{\mathrm{SA}\ (m^2)}{\text{palladium metal weight (g)}} \qquad \text{(Eq. 5)}$$

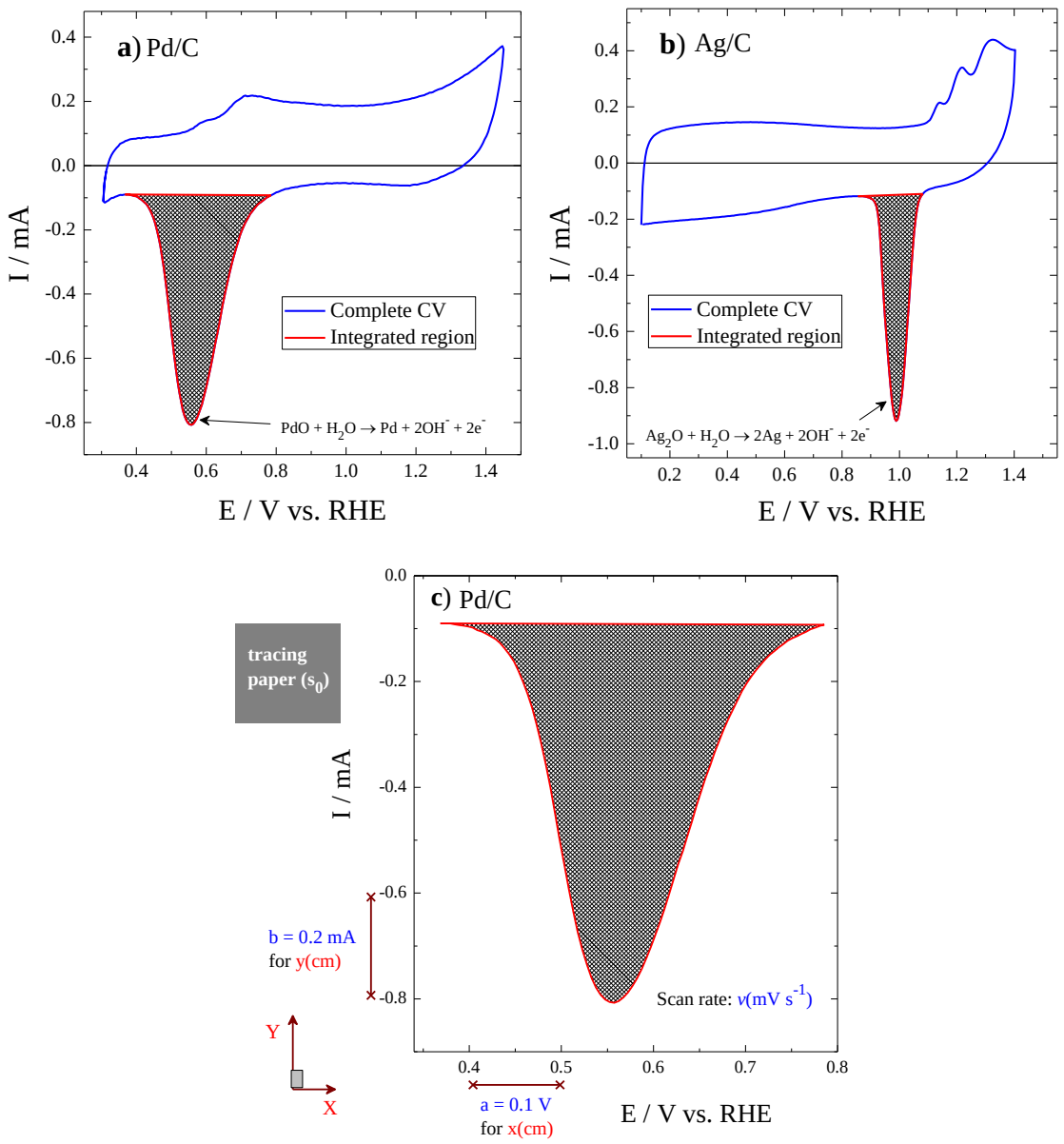

Figure S2: Illustration of the method used for real active surface area evaluation by cyclic voltammetry on Pd/C and b) Ag/C electrode. The blue solid line represents the complete stationary cyclic voltammograms while the shaded curve shows the integrated region. The experiments were recorded in 0.1 mol L^{-1} NaOH at 50 mV s^{-1}. c) An illustration of "weighing method".

4- Effect of scan rate on glycerol electrooxidation at $Pd_{60}Ni_{40}$/C electrode

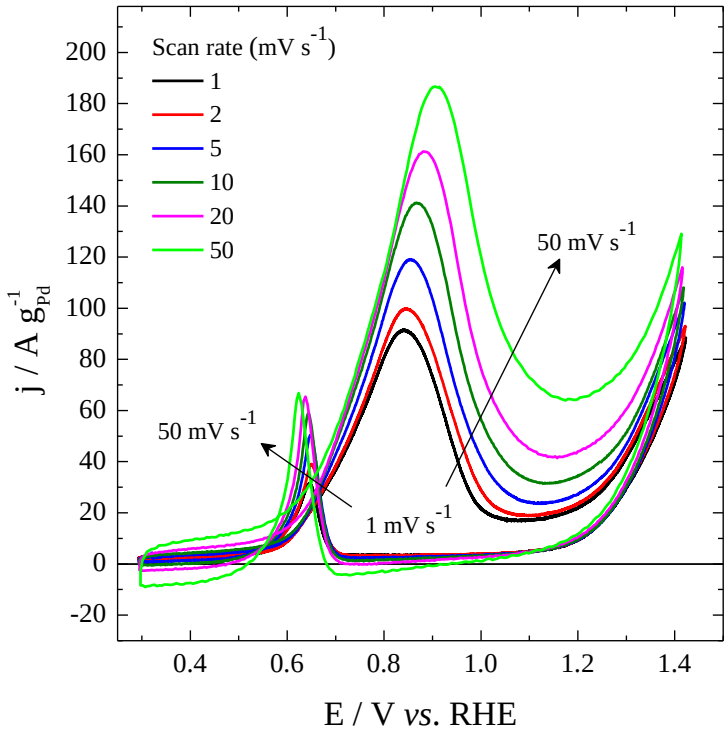

Figure S3: Voltammograms of a $Pd_{60}Ni_{40}$/C electrode recorded at different sweep rates in 0.1 mol L^{-1} NaOH and in the presence of 0.1 mol L^{-1} glycerol.

5- Electrolysis of glycerol

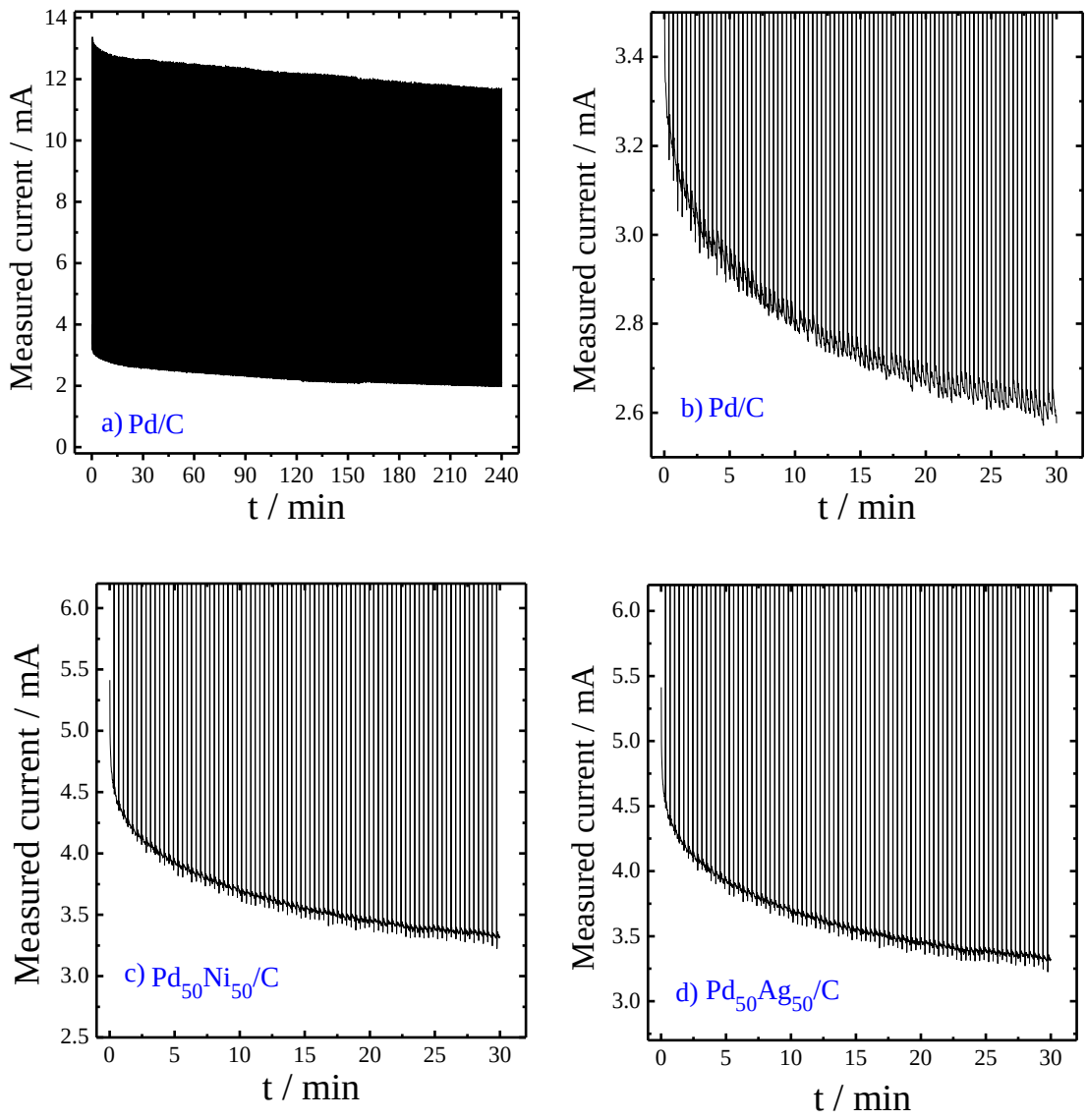

Figure S4: Electrolysis of 0.1 mol L^{-1} glycerol (in 0.1 mol L^{-1} NaOH) on Pd/C: a) Reports the current measured during the 240 min electrolysis; b), c) and d) Current measured during the first 30 min of electrolysis of 0.1 mol L^{-1} of glycerol on Pd/C, $Pd_{50}Ni_{50}$/C and $Pd_{50}Ag_{50}$/C catalysts, respectively.

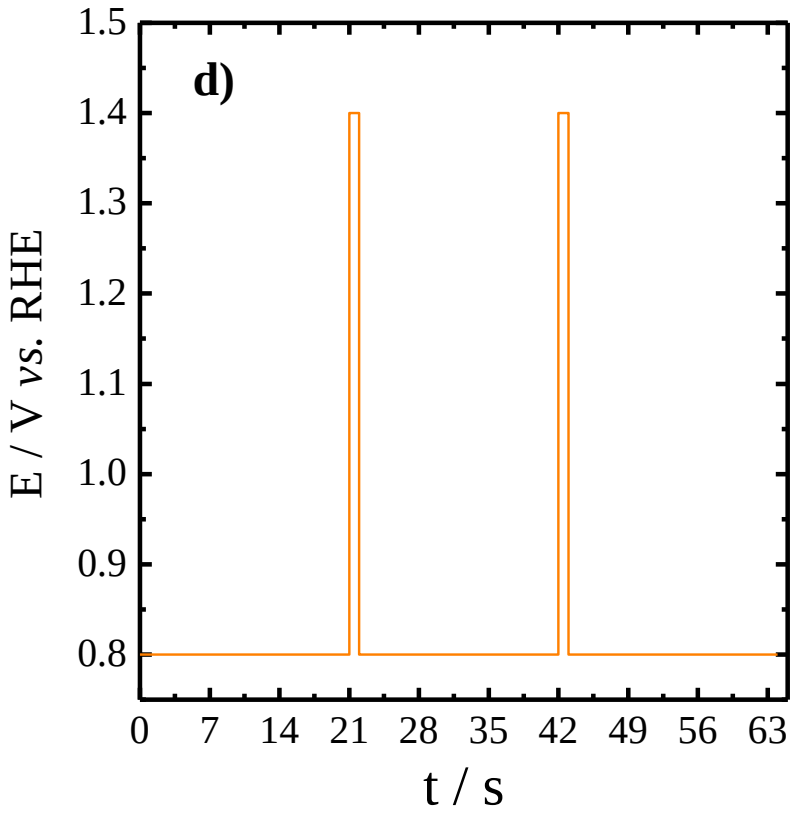

Figure S5: Potential program used for prolonged electrolysis.

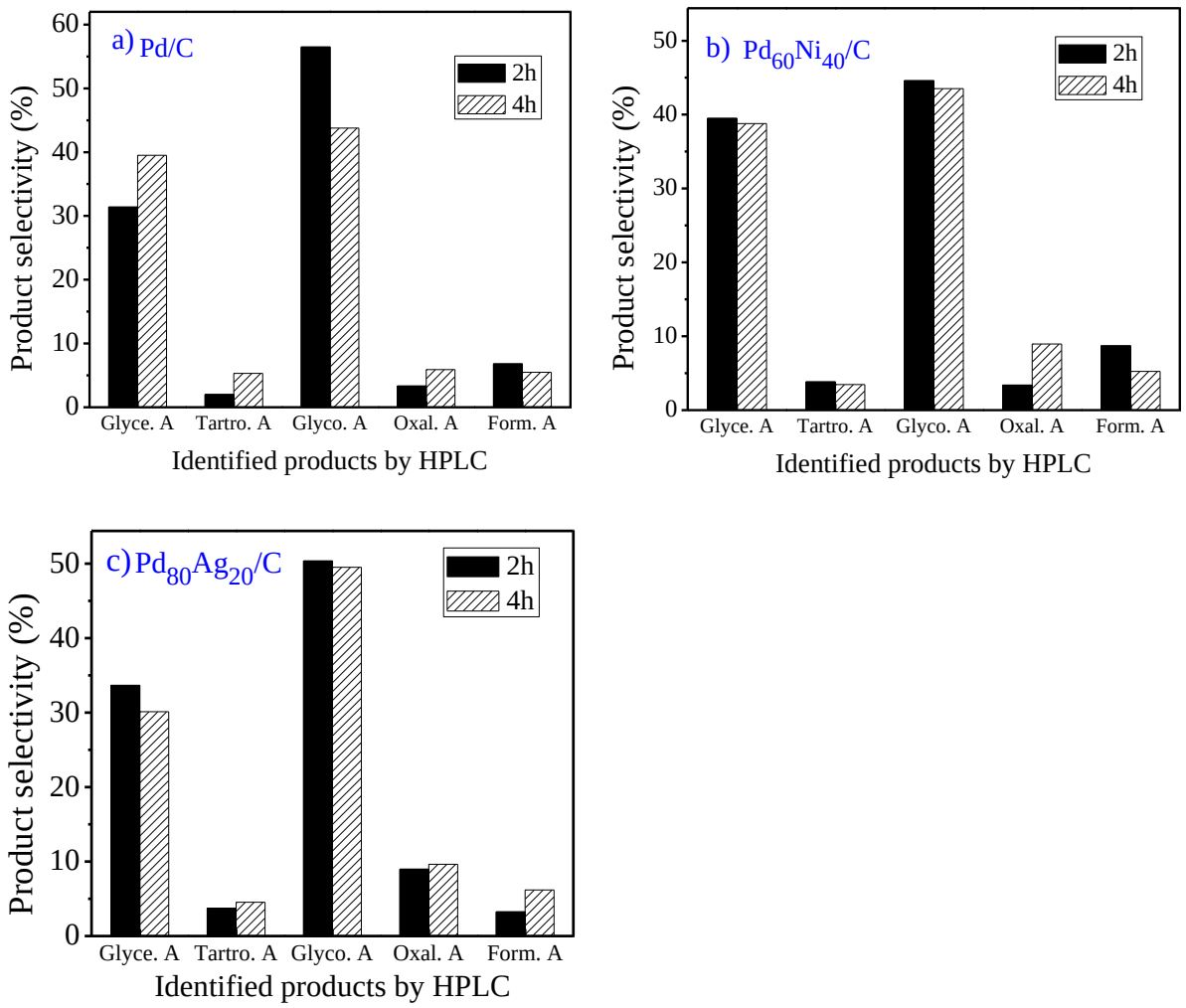

Figure S6: Products distribution on Pd/C (a), $Pd_{60}Ni_{40}/C$ (b) and $Pd_{80}Ag_{20}/C$ (c) catalysts respectively: Glyce. A (Glyceric Acid); Tartro. A (Tartronic Acid); Glyco. A (Glycolic Acid); Oxal. A (Oxalic Acid); Form. A (Formic Acid).

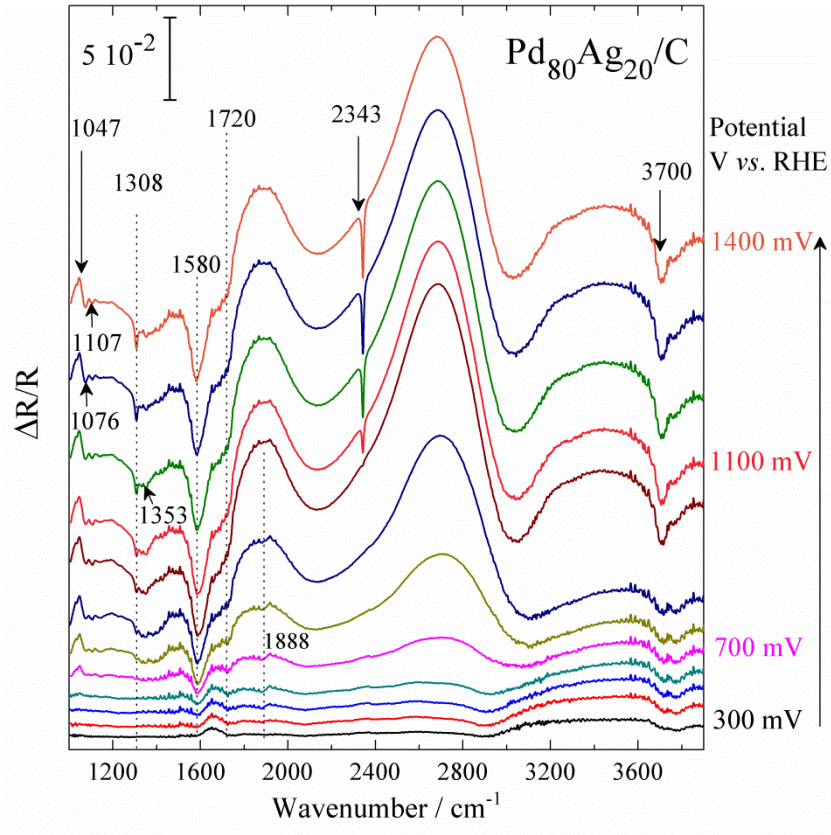

Figure S7: SPAIR spectra recorded in 0.1 mol L^{-1} NaOH electrolyte containing 0.1 mol L^{-1} of glycerol at 1 mV s^{-1} on $Pd_{80}Ag_{20}/C$ catalyst at potentials ranging from 0.30 to 1.45 V *vs*. RHE.

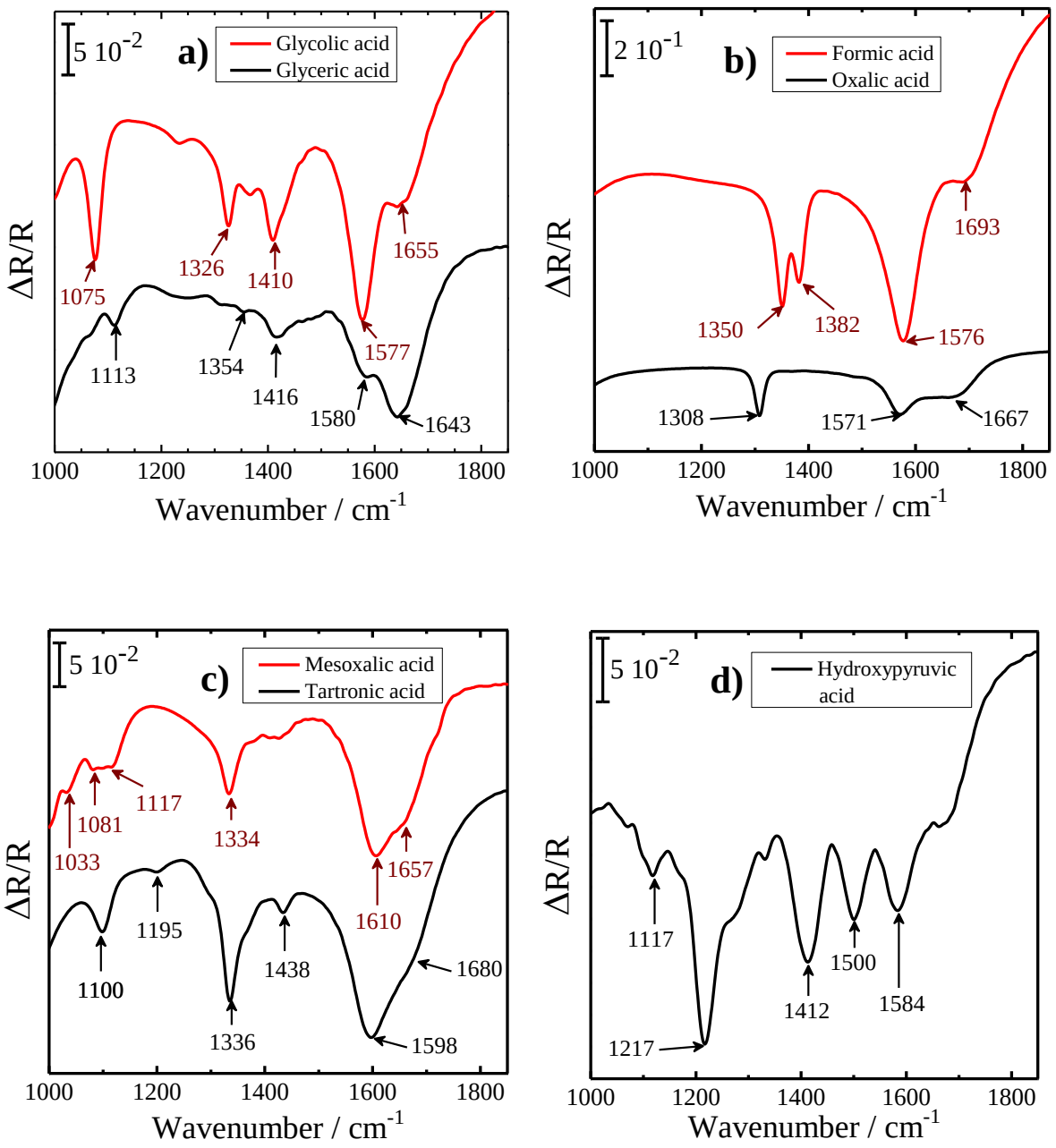

Figure S8: (a-d) Reflectance FTIR spectra of the different possible products or intermediates recorded in 0.1 mol·L^{-1} NaOH aqueous solution.

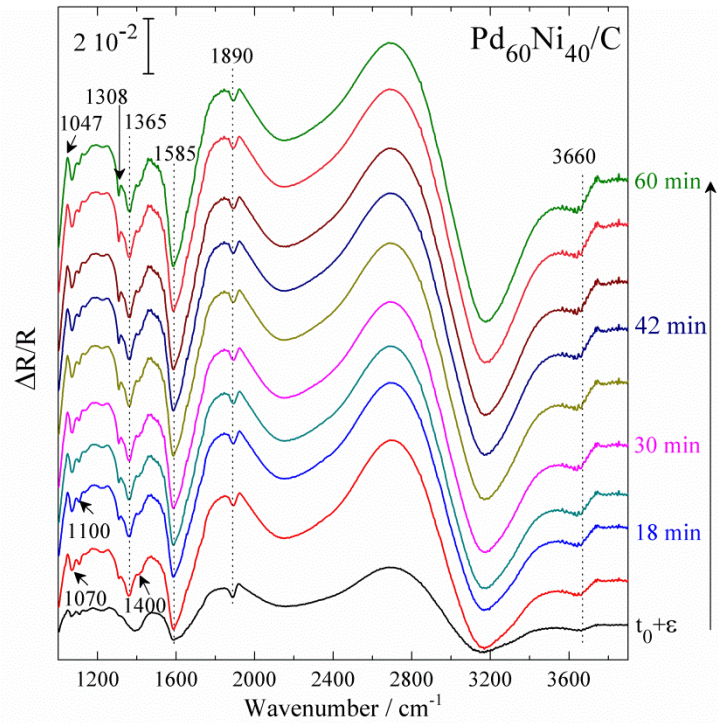

Figure S9: FTIR spectra recorded during chronoamperomety at 0.8 V *vs*. RHE in 0.1 mol L^{-1} NaOH electrolyte containing 0.1 mol L^{-1} of glycerol on PdNi/C catalyst.

References

(1) Trasatti, S.; Petrii, O. A. *J. Electroanal. Chem.* **1992**, *327*, 353.

(2) Herrero, E.; Buller, L. J.; Abruña, H. D. *Chem. Rev.* **2001**, *101*, 1897.

(3) Jerkiewicz, G. *Electrocatal.* **2010**, *1*, 179.

(4) Chen, D.; Tao, Q.; Liao, L.; Liu, S.; Chen, Y.; Ye, S. *Electrocatal.* **2011**, *2*, 207.

(5) Tateishi, N.; Yahikozawa, K.; Nishimura, K.; Takasu, Y. *Electrochim. Acta* **1992**, *37*, 2427.

(6) Jewell, L. L.; Davis, B. H. *Appl. Catal. A: Gen.* **2006**, *310*, 1.

(7) Kobayashi, H.; Yamauchi, M.; Kitagawa, H.; Kubota, Y.; Kato, K.; Takata, M. *J. Am. Chem. Soc.* **2008**, *130*, 1818.

(8) Narehood, D. G.; Kishore, S.; Goto, H.; Adair, J. H.; Nelson, J. A.; Gutiérrez, H. R.; Eklund, P. C. *Int. J. Hydrogen Energy* **2009**, *34*, 952.

(9) Kobayashi, H.; Yamauchi, M.; Kitagawa, H.; Kubota, Y.; Kato, K.; Takata, M. *J. Am. Chem. Soc.* **2010**, *132*, 5576.

(10) Hu, C.-C.; Wen, T.-C. *Electrochim. Acta* **1995**, *40*, 495.

(11) Grden, M.; Lukaszewski, M.; Jerkiewicz, G.; Czerwinski, A. *Electrochim. Acta* **2008**, *53*, 7583.

(12) Simões, M.; Baranton, S.; Coutanceau, C. *J. Phys. Chem. C* **2009**, *113*, 13369.

(13) Maheswari, S.; Sridhar, P.; Pitchumani, S. *Electrocatal.* **2012**, *3*, 13.

(14) Holade, Y.; Morais, C.; Arrii-Clacens, S.; Servat, K.; Napporn, T. W.; Kokoh, K. B. *Electrocatal.* **2013**, *4*, 167.